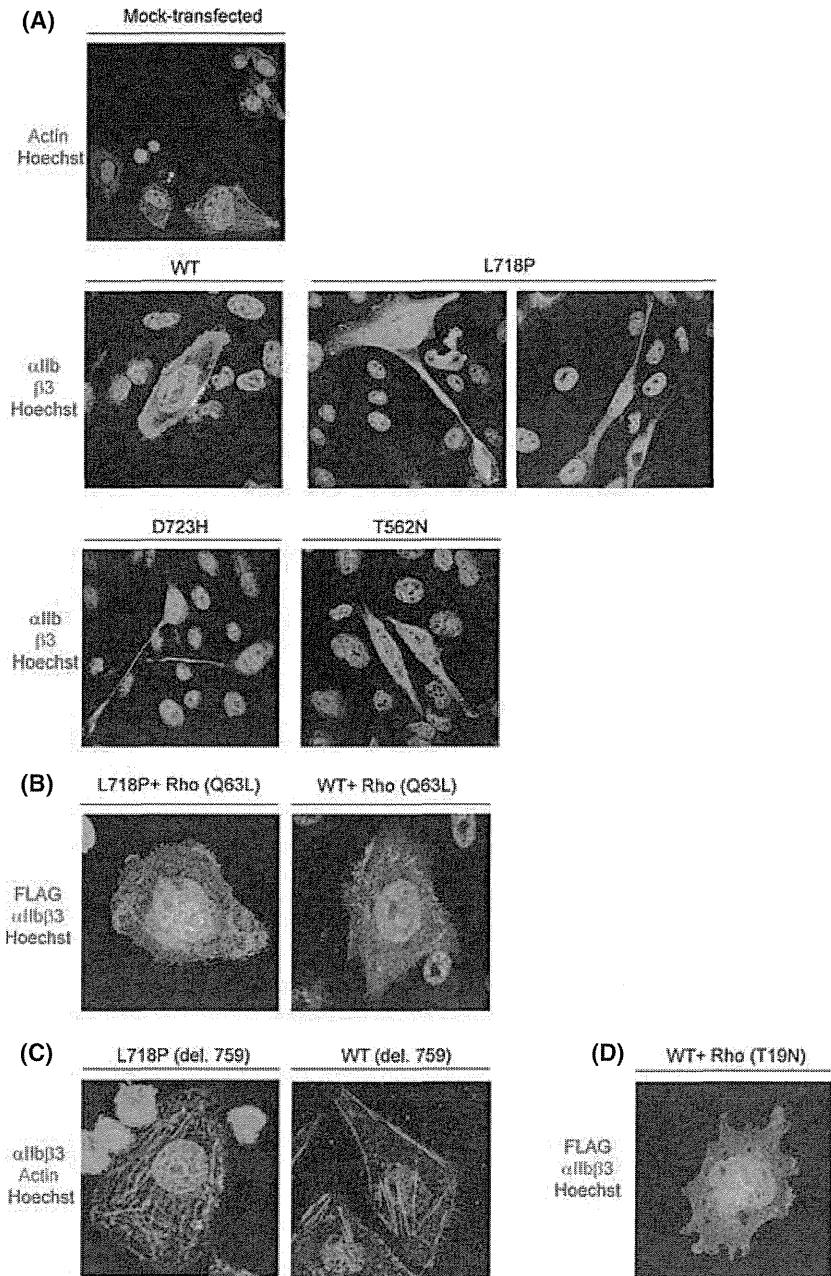


**Fig 3.** Functional analysis of integrin  $\beta_3$ -L718P mutation. (A) Spontaneous binding of PAC-1 antibody to platelets obtained from affected individuals of the pedigree. Non-activated platelets (within 10 min after blood collection), incubated with or without 1 mM RGDS, were stained with FITC-conjugated PAC-1 antibody. After fixation, binding of PAC-1 to platelets was analysed by flow cytometry. Activation status of  $\alpha_{IIb}\beta_3$  complex on resting platelets bound to FITC-PAC-1 (top) and FITC-fibrinogen (bottom). Mean fluorescence intensity (MFI) ratio was estimated by dividing the MFI of resting platelets by that of resting platelets incubated with RGDS. (B) Reduced activation of  $\alpha_{IIb}\beta_3$  from affected individuals. The resting and ADP-stimulated platelets, stained with FITC-conjugated PAC-1 antibody were analysed by flow cytometry. Activation status of  $\alpha_{IIb}\beta_3$  on stimulated platelets bound to FITC-PAC-1 (top) and FITC-fibrinogen (bottom). Values were estimated by dividing the MFI of platelets stimulated with ADP by those of resting platelets. (C) Partial activation of  $\alpha_{IIb}\beta_3$ -L718P and -D723H on CHO cells. CHO cells transfected with  $\alpha_{IIb}\beta_3$  expression vectors ( $\beta_3$ -WT, -L718P, -D723H and -T562N) were seeded on 100  $\mu$ g/ml fibrinogen-coated coverslips in 6-well dishes. The cells, treated with or without RGDS, were stained with FITC-conjugated PAC-1 antibody and PerCP-conjugated anti-CD61 antibody and analysed by flow cytometry. (D) Activation index of  $\alpha_{IIb}\beta_3$  mutants. Activation status of CHO cells expressing  $\alpha_{IIb}\beta_3$ -L718P and -D723H was compared with that of  $\alpha_{IIb}\beta_3$ -T562N as described in the "Materials and methods".



**Fig 4.** Overexpression of RhoA mutants or integrin  $\beta 3$ -L718P (del. 759) modulates the formation of proplatelet-like cell protrusions in CHO cells. (A) Changes in CHO cell morphology by  $\alpha$ IIb $\beta 3$  mutants. CHO cells transfected with  $\alpha$ IIb $\beta 3$ -L718P, -T562N and -D723H were seeded on fibrinogen-coated coverslips. After an 8-h incubation, the cells were fixed and stained with anti-CD41 and -CD61 antibodies followed by staining with Cy3- and Alexa 488-conjugated secondary antibodies. Mock-transfected cells were stained with Alexa 488-conjugated phalloidin and Hoechst 33342. (B) Inhibition of proplatelet-like protrusion formation by constitutively-active RhoA. An expression vector that encodes FLAG-tagged RhoA (Q63L) was transfected together with  $\alpha$ IIb $\beta 3$ -L718P or -WT expressing vectors into CHO cells. The cells grown on fibrinogen-coated coverslips were fixed and stained with anti-CD41 and anti-DDDDK-tag antibodies followed by staining with Alexa 488- and Cy3-conjugated secondary antibodies. (C) C-terminal deletion of  $\beta 3$ -L718P inhibits the formation of proplatelet-like protrusions. C-terminal deleted integrin  $\beta 3$ -L718P or -WT (del. 759) was expressed together with  $\alpha$ IIb in CHO cells. The cells were fixed and stained with anti-CD41 antibody followed by staining with Cy3-conjugated secondary antibody and Alexa-488-labeled phalloidin. (D) A dominant-negative (T19N) form of RhoA was overexpressed in CHO cells. Images were taken as in (B).

*Involvement of RhoA signalling in proplatelet-like protrusion formation*

As previously reported by others (Ghevaert *et al*, 2008; Jayo *et al*, 2010), CHO cells expressing  $\alpha$ IIb $\beta 3$ -L718P, as well as  $\alpha$ IIb $\beta 3$  D723H, formed long proplatelet-like protrusions on fibrinogen-coated dishes that were not observed in cells expressing wild-type  $\alpha$ IIb $\beta 3$  (Fig 4A). In contrast, although cells expressing  $\alpha$ IIb $\beta 3$ -T562N, which yields a fully activated conformation (Kashiwagi *et al*, 1999), changed from their original round shape surrounded by a broad protrusion (Fig 4A, mock-transfected) to rhomboid-like cell morphology, proplatelet-like protrusions were rarely seen (Fig 4A).

This suggests that mutants partially activating the integrin complex induce long proplatelet-like protrusions.

Recently, it was reported that the formation of proplatelet-like protrusions in CHO cells is mediated by the downregulation of RhoA activity (Chang *et al*, 2007; Schaffner-Reckinger *et al*, 2009), which is initiated by the binding of c-Src to the C-terminal tail (amino acid 760–762, Arg-Gln-Thr; RGT) of integrin  $\beta 3$  (Flevaris *et al*, 2007). We found that the formation of long cell protrusions was inhibited when a constitutively-active form of RhoA (Q63L) was introduced into  $\alpha$ IIb $\beta 3$ -L718P-expressing cells (Fig 4B). In addition, CHO cells expressing  $\alpha$ IIb $\beta 3$ -L718P (del. 759) mutant, which lacks the C-terminal c-Src binding site of in-

tegrin  $\beta 3$  (RGT), did not form any proplatelet-like protrusions (Fig 4C). Given that enforced activation of RhoA caused by introducing RhoA (Q63L), as well as de-repression of RhoA through C-terminal deletion of  $\beta 3$  in cells expressing  $\alpha IIb\beta 3$ -WT, did not induce morphological changes in CHO cells (Figs 4B, C), it is proposed that constitutive inhibition but not activation through the c-terminal of  $\beta 3$  is responsible for the formation of abnormal cell protrusions in L718 mutants. However, as the enforced expression of a dominant negative form of RhoA (T19N) in  $\alpha IIb\beta 3$ -WT expressing cells did not result in typical proplatelet-like protrusions (Fig 4D), this suggests that downregulation of RhoA was required but not sufficient for the formation of proplatelet-like protrusions induced by integrin  $\beta 3$ -L718P.

## Discussion

We report a pedigree with individuals suffering from a lifelong haemorrhagic syndrome, all of whom were carrying the integrin  $\beta 3$ -L718P mutation. This had previously been reported only in a sporadic patient (Jayo *et al*, 2010). Next-generation sequencing, together with the clinical data of the patients, established that this integrin  $\beta 3$ -L718P mutation causes thrombocytopenia resembling the disease caused by a different integrin mutation,  $\beta 3$ -D723H, although the size of the platelets seems to differ somewhat between these mutations (Ghevaert *et al*, 2008; Schaffner-Reckinger *et al*, 2009).

Considering the dominant inheritance pattern of the haemorrhagic tendency caused by integrin  $\beta 3$ -L718P as well as  $\beta 3$ -D723H, these would be gain of function mutations, unlike those causing Glanzmann thrombasthenia. Indeed, expression of integrin  $\beta 3$ -D723H partially activates the  $\alpha IIb\beta 3$  complex, resulting in downregulation of RhoA activity and induction of microtubule-dependent proplatelet-like cell protrusions considered relevant for production of macrothrombocytes (Ghevaert *et al*, 2008; Schaffner-Reckinger *et al*, 2009). Integrin  $\beta 3$ -L718P appears to act in a similar fashion (Fig 4A and B). Interestingly, we demonstrate that the three C-terminal amino acid residues (RGT) of integrin  $\beta 3$  are required for L718P to form proplatelet-like cell protrusions (Fig 4C). RGT provides a binding site for c-Src tyrosine kinase, which was shown to inactivate RhoA (Flevaris *et al*, 2007), further supporting the hypothesis that

integrin  $\beta 3$ -L718P plays a role in causing megakaryocytes to produce abnormal platelets through the inhibition of RhoA.

In platelets derived from megakaryocytes that carry the integrin  $\beta 3$ -L718P mutation, full activation of  $\alpha IIb\beta 3$  complex in response to inside-out stimuli is inhibited, as shown by reduced binding of PAC-1 and fibrinogen on stimulation with ADP (Fig 3B). A simple scenario is that, in platelets, integrin  $\beta 3$ -L718P acts as a loss of function mutation. However, given that the carriers of Glanzmann's thrombasthenia who have both normal and mutant allele and express reduced amounts of the  $\alpha IIb\beta 3$  complex, in general show normal platelet aggregation, it is possible that the integrin  $\beta 3$ -L718P mutation gains a function that ultimately results in the reduction of inside-out signals.

In summary, identification of a pedigree showing autosomal dominant inheritance leads to a model whereby the integrin  $\beta 3$ -L718P mutation contributes to thrombocytopenia accompanied by anisocytosis most likely through gain-of-function mechanisms. Further investigations are necessary to fully elucidate these mechanisms by which this mutation exerts its abnormal effect on thrombocytosis and platelet aggregation.

## Acknowledgements

We thank Prof. M. Matsumoto and Ms. M. Sasatani for providing clinical data; Ms. M. Nakamura, Ms. E. Kanai and Ms. R. Tai for excellent technical assistance. This work was partly supported by Grants-in-Aid for Scientific Research from the Ministry of Health, Labour and Welfare of Japan.

## Author contributions

H.M., T.I. and M.K. designed the work. Y.K., H.M., A.K., S.O. and M.T. performed experiments and analysed data. S.K. contributed essential materials and interpreted data. M.M. and K.N. contributed clinical materials and data. H.M., Y.K. and T.I. wrote the manuscript.

## Conflict of interest

The authors declare no competing financial interests.

## References

- Chang, Y., Auradé, F., Larbret, F., Zhang, Y., Couedic, J.P.L., Momeux, L., Larghero, J., Bertoglio, J., Louache, F., Cramer, E., Vainchenker, W. & Debili, N. (2007) Proplatelet formation is regulated by the Rho/ROCK pathway. *Blood*, **109**, 4229–4236.
- Flevaris, P., Stojanovic, A., Gong, H., Chishti, A., Welch, E. & Du, X. (2007) A molecular switch that controls cell spreading and retraction. *Journal of Cell Biology*, **179**, 553–565.
- George, J.N., Caen, J.P. & Nurden, A.T. (1990) Glanzmann's thrombasthenia: the spectrum of clinical disease. *Blood*, **75**, 1383–1395.
- Ghevaert, C., Salsmann, A., Watkins, N.A., Schaffner-Reckinger, E., Rankin, A., Garner, S.F., Stephans, J., Smith, G.A., Debili, N., Vainchenker, W., de Groot, P.G., Huntington, J.A., Laffan, M., Kieffer, N. & Ouwehand, W.H. (2008) A non-synonymous SNP in the ITGB3 gene disrupts the conserved membrane-proximal cytoplasmic salt bridge in the  $\alpha IIb\beta 3$  integrin and cosegregates dominantly with abnormal proplatelet formation and macrothrombocytopenia. *Blood*, **111**, 3407–3414.
- Hughes, P.E., Diaz-Gonzalez, F., Leong, L., Wu, C., McDonald, J.A., Shattil, S.J. & Ginsberg, M.H. (1996) Breaking the integrin hinge. A defined structural constraint regulates integrin signaling. *Journal of Biological Chemistry*, **271**, 6571–6574.
- Jayo, A., Conde, I., Lastres, P., Martinez, C., Rivera, J., Vicente, V. & Manchón, C.G. (2010) L718P mutation in the membrane-proximal

- cytoplasmic tail of  $\beta 3$  promotes abnormal  $\alpha \text{IIb}\beta 3$  clustering and lipid domain coalescence, and associates with a thrombasthenia-like phenotype. *Haematologica*, **95**, 1158–1166.
- Kashiwagi, H., Tomiyama, Y., Tadokoro, S., Honda, S., Shiraga, M., Mizutani, H., Honda, M., Kurata, Y., Matsuzawa, Y. & Shattil, S.J. (1999) A mutation in the extracellular cysteine-rich repeat region of the  $\beta 3$  subunit activates integrins  $\alpha \text{IIb}\beta 3$  and  $\alpha \text{V}\beta 3$ . *Blood*, **93**, 2559–2568.
- Kunishima, S., Kashiwagi, H., Otsu, M., Takayama, N., Eto, K., Onodera, M., Miyajima, Y., Takamatsu, Y., Suzumiya, J., Matsubara, K., Tomiyama, Y. & Saito, H. (2011) Heterozygous ITGA2B R995W mutation inducing constitutive activation of the  $\alpha \text{IIb}\beta 3$  receptor affects proplatelet formation and causes congenital macrothrombocytopenia. *Blood*, **117**, 5479–5484.
- Nurden, A.T. (2006) Glanzmann thrombasthenia. *Orphanet Journal of Rare Diseases*, **1**, 10.
- Nurden, P. & Nurden, A.T. (2008) Congenital disorders associated with platelet dysfunctions. *Thrombosis and Haemostasis*, **99**, 253–263.
- Nurden, A.T., Fiore, M., Nurden, P. & Pillois, X. (2011a) Glanzmann thrombasthenia: a review of ITGA2B and ITGB3 defects with emphasis on variants, phenotype variability, and mouse models. *Blood*, **118**, 5996–6005.
- Nurden, A.T., Pillois, X., Fiore, M., Heilig, R. & Nurden, P. (2011b) Glanzmann thrombasthenia-like syndromes associated with macrothrombocytopenias and mutations in the gene encoding the  $\alpha \text{IIb}\beta 3$  integrin. *Seminars in Thrombosis and Hemostasis*, **37**, 698–706.
- Schaffner-Reckinger, E., Salsmann, A., Debili, N., Bellis, J., Demey, J., Vainchenker, W., Ouwehand, W.H. & Kieffer, N. (2009) Overexpression of the partially activated  $\alpha \text{IIb}\beta 3 \text{D723H}$  integrin salt bridge mutant downregulates RhoA activity and induces microtubule-dependent proplatelet-like extensions in Chinese hamster ovary cells. *Journal of Thrombosis and Haemostasis*, **7**, 1207–1217.
- Shattil, S.J., Cunningham, M. & Hoxie, J.A. (1987) Detection of activated platelets in whole blood using activation-dependent monoclonal antibodies and flow cytometry. *Blood*, **70**, 307–315.

## Regulation of hematopoietic stem cells using protein transduction domain–fused Polycomb

Teruyuki Kajiume<sup>a</sup>, Yasuhiko Sera<sup>a</sup>, Yumi Kawahara<sup>b</sup>, Masaya Matsumoto<sup>b</sup>, Takahiro Fukazawa<sup>b</sup>, Takeshi Imura<sup>b</sup>, Louis Yuge<sup>b</sup>, and Masao Kobayashi<sup>a</sup>

<sup>a</sup>Department of Pediatrics, Graduate School of Biomedical Sciences, Hiroshima University, Hiroshima, Japan; <sup>b</sup>Division of Bio-Environmental Adaptation Sciences, Graduate School of Health Sciences, Hiroshima University, Hiroshima, Japan

(Received 9 November 2011; revised 7 May 2012; accepted 16 May 2012)

The Polycomb-group complex is a chromatin regulatory factor that is classified into two different complexes: Polycomb repressive complex 1 and 2. Components of Polycomb repressive complex 1 are involved in the self-renewal of hematopoietic stem cells. *Bmi1*, one of these components, maintains the immaturity of neural and cancer stem cells as well as that of hematopoietic stem cells. We constructed recombinant protein transduction domain (PTD)-Polycomb proteins and transduced them into murine bone marrow (BM) cells. We designed and fused the PTD-protein transduction domain to three proteins (i.e., green fluorescent protein, *Bmi1*, and *Mel18*). Murine BM cells were incubated for 48 h and each PTD-Polycomb protein was added. Then, we analyzed the function of hematopoiesis using the colony assay and transplantation. BM cells exposed to PTD-*Bmi1* showed an increased number of colonies. In contrast, BM cells exposed to PTD-*Mel18* or to both proteins showed a decreased number of colonies. Hematopoietic cells derived from PTD-*Bmi1*-transduced BM cells were significantly increased in the peripheral blood at 6 weeks after transplantation. Moreover, 80% of mice transplanted with PTD-*Bmi1*-transduced BM cells died at 8 to 24 weeks after transplantation. However, only a few early deaths were observed in the mice transplanted with BM cells exposed to both PTD-*Bmi1* and PTD-*Mel18*. We expect that hematopoietic stem cells could proliferate after transduction with PTD-*Bmi1*, but this may generate undesirable effects, e.g., tumorigenesis. Thus, *Bmi1* and *Mel18* have opposing functions and are present in distinct complexes. © 2012 ISEH - Society for Hematology and Stem Cells. Published by Elsevier Inc.

*Polycomb-group* genes encode molecules that form the Polycomb-group complex, which is involved in the methylation and ubiquitylation of histones [1–4]. The Polycomb-group complex is a chromatin regulatory factor that includes two types of complexes: Polycomb repressive complex (PRC) 1 and PRC2 [5–9]. The components of PRC1 are involved in the self-renewal of hematopoietic stem cells (HSCs) in mammals [10–14]. *Bmi1*, one of these components, maintains the immaturity of neural and cancer stem cells as well as that of HSCs [15–20]. However, *BM1* is also involved in the malignancy of cancer cells, and

a relationship between *BM1* expression and prognosis has been reported for various types of tumors [21–24]. *BM1* is related to tumorigenesis as well as to the immaturity of cells.

The *Mel18* protein is composed of 342 amino acids, and the *N*-terminal region of the 102<sup>nd</sup> amino acid, which includes the really interesting new gene (RING) finger motif and shares 93% homology with the *Bmi1* protein [25]. In addition, the secondary structure of this region shows a high homology with the *Mel18* and *Bmi1* proteins. Many studies have shown that *mel18*, which has 90% homology to *bmi1*, has opposing functions to *bmi1* [26–29]. We previously reported that *mel18* is necessary for the differentiation of murine HSCs, and not for their self-renewal, in experiments using knockout mice and gene knockdown with RNA interference (RNAi) [13]. This function of *mel18* is the opposite to that of *bmi1*. Moreover, we reported that *bmi1* and *mel18* act reciprocally in HSCs [14].

Offprint requests to: Teruyuki Kajiume, M.D., Ph.D., Department of Pediatrics, Graduate School of Biomedical Sciences, Hiroshima University, 1-2-3 Kasumi, Minami-ku, Hiroshima 734-8551, Japan; E-mail: kajiume@hiroshima-u.ac.jp

Supplementary data related to this article can be found online at <http://dx.doi.org/10.1016/j.exphem.2012.05.005>.

In protein transduction, high molecular-weight target proteins are induced into cells by fusing them with peptides called protein transduction domains (PTDs), such as HIV tat and polyarginine [30,31]. An innovative study showed the induction of self-renewal in murine HSCs using a recombinant TAT-HoxB4 protein [32]. Furthermore, Zhou et al. recently reported the successful establishment of induced pluripotent stem cells using a recombinant protein fused with polyarginine [33].

In this study, we constructed recombinant PTD-Polycomb proteins and transduced them into murine HSCs. Although the transduced HSCs showed potential symptoms of tumorigenesis, our results indicate that the transduced *Bmi1* or *Mel18* may regulate the self-renewal or differentiation of HSCs without gene transduction.

## Materials and methods

### Mice

We used 5- to 8-week-old C57BL/6 mice (Ly5.1 or Ly5.2). Ly5.1 mice were obtained from The Sankyo Labo Service Corporation (Tokyo, Japan). All mice were bred and maintained in the animal facility at Hiroshima University.

### Cells

**Collection of murine bone marrow cells.** Bone marrow (BM) was flushed from the medullary cavities of murine bones using phosphate-buffered saline.

**Murine erythroleukemia cells.** Murine erythroleukemia (MEL) cells were cultured in RPMI-1640 medium supplemented with 10% fetal bovine serum and 2% penicillin/streptomycin.

### Preparation of the Polycomb expression vector, protein extraction, and purification

Full-length *bmi1* and *mel18* complementary DNAs were generated by real-time reverse transcriptase polymerase chain reaction (PCR) (ReverTra Ace and KOD plus; TOYOBO Co., Ltd., Osaka, Japan) from messenger RNA extracted from murine BM cells. Restriction enzyme sites were created on both ends of the PCR primers. To generate recombinant proteins that could penetrate the plasma membrane, we designed and fused a TAT peptide to the *N*-terminus or a polyarginine protein transduction domain to the *C*-terminus of three proteins (i.e., green fluorescent protein [GFP], *Bmi1*, and *Mel18*). The TAT and the polyarginine peptides enabled the recombinant proteins to enter the cells and allowed their translocation into the nucleus. *GFP*, *bmi1*, and *mel18* complementary DNAs were cloned into the pET47 expression plasmid (Merck KGaA, Darmstadt, Germany). The plasmids were transformed into *Escherichia coli* BL21 (DE3). Cells were grown in LB medium with kanamycin at 37°C using the Overnight Express Autoinduction System (Merck). His-tagged proteins were purified using TALON metal affinity resin (BD Biosciences, San Jose, CA, USA) according to the manufacturer's instructions.

### Addition of PTD-Polycomb proteins

We added 20 ng/mL solution of the human *flt3* ligand (PeproTech, London, UK) and human thrombopoietin (Kirin Brewery Co.,

Tokyo, Japan) to Dulbecco's modified Eagle's medium containing a supplement (StemPro 34; Invitrogen Inc., San Diego, CA, USA). The initial concentration of BM cells was  $1.0 \times 10^6$  cells/mL. The culture plates were incubated at 37°C for 48 h in a humidified atmosphere with 5% CO<sub>2</sub>. Each PTD-Polycomb protein was added at a final concentration of 50 nM. We introduced each PTD-Polycomb protein into our cell cultures every 6 h.

### Flow cytometry analysis

To analyze the primitive hematopoietic cells, the collected cells were labeled with an antibody cocktail consisting of biotinylated anti-Gr1, anti-Mac1, anti-B220, anti-CD4, anti-CD8, and anti-Ter119 mouse antibodies. The cells were stained with phycoerythrin-conjugated anti-Sca1, allophycocyanin-conjugated anti-*c*-Kit, and streptavidin-conjugated peridinin-chlorophyll-protein complex. All antibodies were purchased from BD Pharmingen (San Diego, CA, USA). Dead cells stained with propidium iodide were excluded from the analysis. Flow cytometry analysis was performed on a FACSCaliber system (BD Biosciences, Bedford, MA, USA).

### Western blot analysis

The MEL cells that were exposed to PTD-Polycomb proteins were separated into the nuclear and cytosolic fractions. For fractionation, a Nuclear/Cytosol Fractionation Kit (BioVision Inc., Mountain View, CA, USA) was used according to the manufacturer's protocol.

After 48 h of coculturing MEL cells with PTD-Polycomb proteins, His-tagged Polycomb proteins were extracted using TALON metal affinity resin (BD Biosciences). Cell extracts were used as samples for the pull-down assays.

Protein extracts were subjected to sodium dodecyl sulfate polyacrylamide gel electrophoresis and immunoblotting. The blot was removed from the transfer apparatus and blocked overnight at 4°C in Tris-buffered saline-Tween 20. The blot was washed three times in Tris-buffered saline-Tween 20 after the overnight incubation. We used the following primary antibodies: mouse monoclonal antibodies against Ring1 and *Bmi1* (Millipore Corporation, Billerica, MA, USA), a goat polyclonal antibody against *Mel18* (Abcam, Cambridge, UK), and a mouse monoclonal antibody against the 6x His synthetic peptide (Abcam). Chemiluminescence was detected using ECL plus Western blotting detection reagents (GE Healthcare UK Ltd, Little Chalfont, UK).

### Quantitative reverse transcriptase PCR

To analyze the influence of PTD-Polycomb proteins, we performed reverse transcription using ExScript reverse transcriptase and SYBR Premix Ex Taq (TAKARA BIO Inc., Shiga, Japan) according to manufacturer's protocol. Real-time PCR was used for the quantitative analysis of gene expression (Opticon; Bio-Rad Laboratories, Hercules, CA, USA). The following specific primers were used: mouse *cdkn2a* (*ink4a*), sense primer 5'-CGA TTC AGG TGA TGA TGA TGG-3' and antisense primer 5'-CAG CGT GTC CAG GAA GC-3'; and mouse *actb*, sense primer 5'-CAT CCG TAA AGA CCT CTA TGC CAA C-3' and antisense primer 5'-ATG GAG CCA CCG ATC CAC A-3'.

### Methylcellulose colony assay

In vitro colony-forming cell activity was assessed by performing a methylcellulose colony assay. BM cells (1000 cells/well) were cultured in a methylcellulose medium containing various

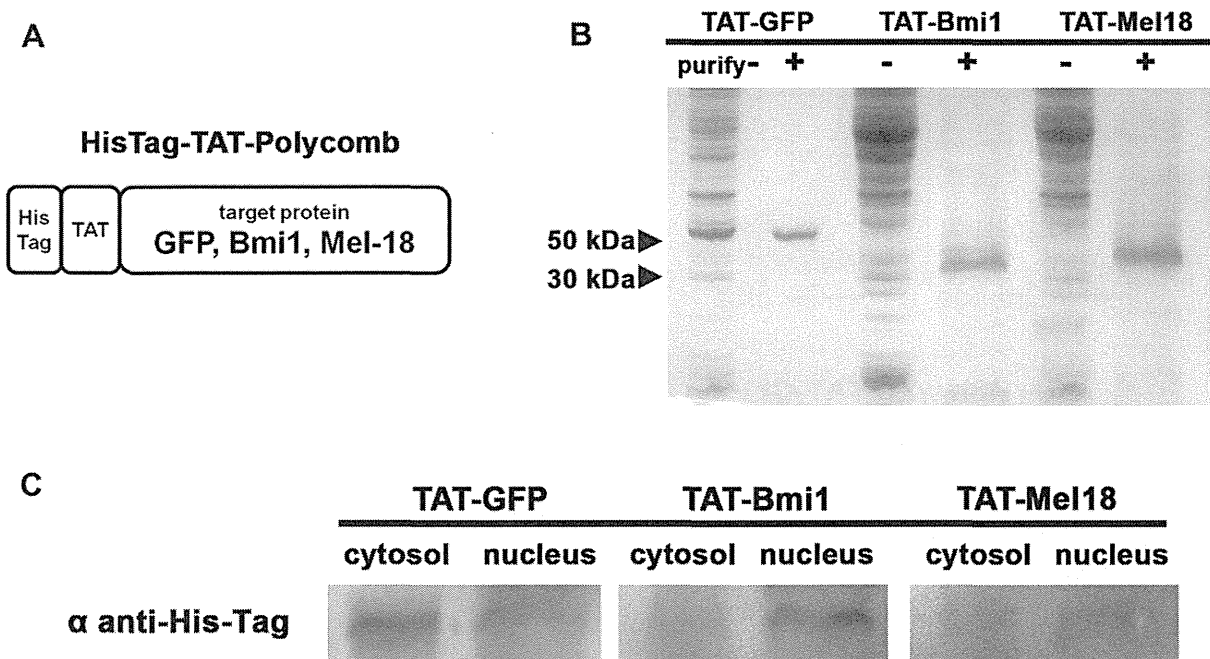


**Figure 1.** Preparation of recombinant TAT-Polycomb proteins. (A) *bmi1*, *mel18*, and *GFP* genes were fused with a HisTag and TAT at their *N*-terminus. (B) The recombinant TAT-Polycomb proteins were purified. Proteins were separated using sodium dodecyl sulfate polyacrylamide gel electrophoresis, and the polyacrylamide gel was stained with Coomassie brilliant blue. (C) Purified TAT-Polycomb was added to cultures of MEL cells. The MEL cells were separated into the nuclear and cytosolic fractions. GFP was detected more often in the cytosol than in the nucleus. Bmi1 and Mel18 were detected exclusively in the nucleus.

cytokines (Methocult GF M3434; StemCell Technologies, Vancouver, BC, Canada). The culture plates were incubated at 37°C for 7 days in a humidified atmosphere with 5% CO<sub>2</sub>. A colony was defined as a group of >50 cells. Erythroid, myeloid, and mixed erythroid-myeloid colonies were counted using an inverted microscope. A secondary colony-forming cell assay was performed by replating aliquots of the cells obtained by harvesting complete primary colonies. The secondary colonies were counted after an additional week of incubation.

#### *In vivo* BM transplantation assay

We performed a transplantation experiment in which the recipient mice were F1 hybrids of Ly5.1 and Ly5.2 mice. Donor and competitor cells ( $2.0 \times 10^5$  cells each) were intravenously transplanted into F1 recipients that were lethally irradiated with a dose of 9 Gy (rate, 1 Gy/min). Four donor and four competitor mice were used for each marrow transplantation experiment. Eight to 12 mice were used as the recipient mice for each BM transplantation experiment. For the donor Ly5.2 cells, each cell was exposed to PTD-Polycomb proteins before being analyzed, and the competitor Ly5.1 cells were exposed to PTD-GFP. Peripheral blood samples were collected from the recipient mice every 4 weeks after transplantation. To distinguish between the 2 competing transplant cell populations, we stained the cells with phycoerythrin-conjugated anti-Ly5.1 and allophycocyanin-conjugated anti-Ly5.2. All antibodies were purchased from Abcam.

#### Statistical analysis

Data are presented as the mean  $\pm$  standard error, unless otherwise stated. Student's *t* test was applied. Differences of  $p < 0.05$  were considered statistically significant.

## Results

#### Preparation of recombinant PTD-Polycomb proteins

We manipulated the *bmi1*, *mel18*, and *GFP* genes such that they were fused to a HisTag and TAT at their *N*-terminus or a polyarginine at their *C*-terminus and inserted the designed genes into pET plasmids (Fig. 1A, Supplementary Figure E1A; online only, available at [www.exphem.org](http://www.exphem.org)). These pET plasmids were transformed into DE3 cells, and the recombinant PTD-Polycomb proteins were purified as described previously (Fig. 1B, Supplementary Figure E1B; online only, available at [www.exphem.org](http://www.exphem.org)). Most GFP proteins form dimers because of their high concentrations. Purified PTD-Polycomb was added to cultures of MEL cells. The MEL cells were separated into their nuclear and cytosolic fractions after 6 h of culture, and the distribution of the PTD-Polycomb proteins was analyzed. GFP was detected more often in the cytosol than in the nucleus. Bmi1 and Mel18 were detected exclusively in the nucleus (Fig. 1C, Supplementary Figure E1C; online only, available at [www.exphem.org](http://www.exphem.org)). These results indicate that PTD-Polycomb proteins can be translocated to the nucleus after their addition to the culture medium.

#### Flow cytometry profile of recombinant TAT-Polycomb protein-transduced murine BM cells

We performed flow cytometry analysis of murine BM cells exposed to recombinant TAT-Polycomb proteins for 48 h.

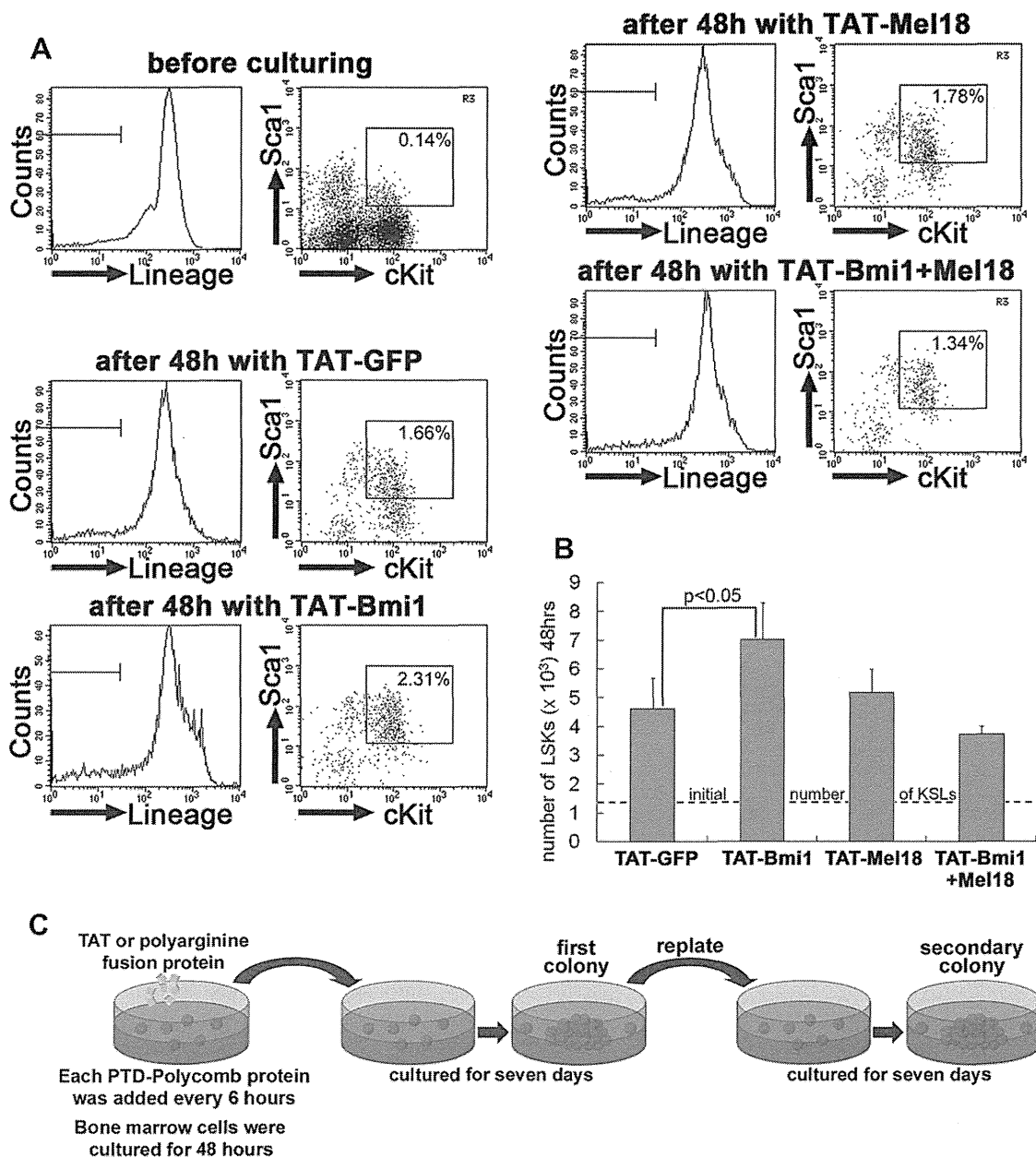


**Figure 2.** In vitro colony assay of recombinant TAT-Polycomb protein-transduced murine bone marrow (BM) cells. (A) The initial ratio of LSK cells from BM of fresh mice was  $\sim 0.14\%$ . The ratio of LSK cells was increased when TAT-Bmi1 was added in BM cells and cultured for 48 h compared with the other recombinant proteins. (B) In comparison with the total cell number, the number of LSK cells was significantly increased following the addition of TAT-Bmi1. In addition to TAT-Mel18 alone, or the addition of both TAT-Bmi1 and TAT-Mel18, the number of LSK cells was not significantly increased compared with TAT-GFP. (C) Recombinant TAT-Polycomb proteins were added during the first 48 h of culturing. A methylcellulose colony assay was performed using marrow cells to which each protein was added. Then, the secondary colony-forming potential of the cells was assayed.

Because the lineage marker-negative, Sca-1-positive, and c-Kit-positive (LSK) cells possess the highest long-term multilineage reconstitution activity [34,35], we used this population for these experiments. The ratio of LSK cells from murine BM was  $0.14\%$ . The ratio of LSK cells increased when TAT-Bmi1 was added to BM cells and cultured for 48 h compared to the addition of other fused proteins (Fig. 2A). The initial concentration of BM cells was  $1.0 \times 10^6$  cells/mL; the number of LSK cells was

significantly increased after the addition of TAT-Bmi1. In addition to TAT-Mel18 alone, or the addition of both TAT-Bmi1 and TAT-Mel18, the number of LSK cells was not increased compared with TAT-GFP (Fig. 2B).

#### *In vitro colony assay of recombinant TAT-Polycomb protein-transduced murine BM cells*

We performed a secondary colony assay to assess primitive hematopoiesis [13,14]. The secondary colony-forming



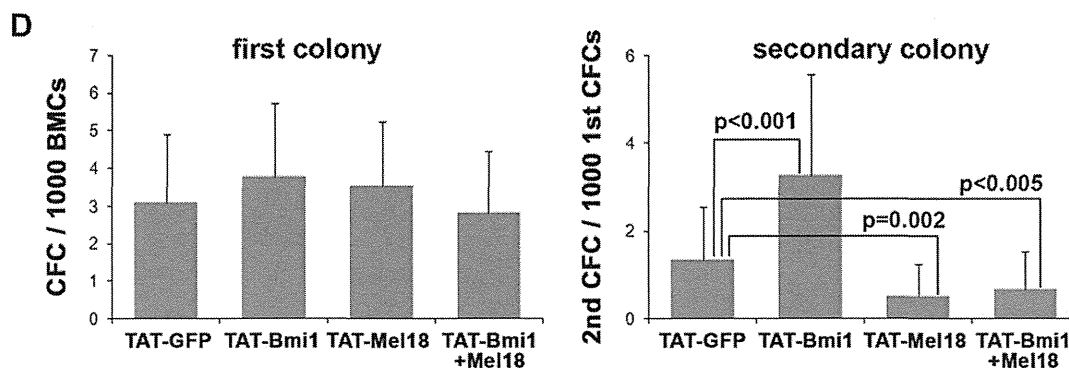


**Figure 2.** (Continued) (D) There was no significant difference in primary colony-forming potential between the recombinant proteins. However, BM cells exposed to recombinant TAT-Bmi1 showed an increased number of secondary colonies. In contrast, BM cells exposed to recombinant TAT-Mel18 or to both proteins showed a decreased number of secondary colonies.

potential of murine BM cells exposed to recombinant TAT-Polycomb proteins at a final concentration of 50 nM for 48 h was assayed (Fig. 2C). There were no significant differences in the primary colony-forming potential between the recombinant proteins. There was no significant difference in the classification of the colonies (e.g., colony-forming unit granulocyte-macrophage, burst-forming unit erythroid), even when TAT-Polycomb protein was added. However, BM cells exposed to recombinant TAT-Bmi1 showed an increased number of secondary colonies. In contrast, BM cells exposed to recombinant TAT-Mel18 or to both recombinant proteins showed a decreased number of secondary colonies (Fig. 2D). Similar results were obtained for recombinant polyarginine-Polycomb (Supplementary Figure E2; online only, available at [www.exphem.org](http://www.exphem.org)). These results suggest that Mel18 may attenuate the potential of Bmi1 to increase the formation of secondary colonies.

#### *In vivo* BM transplantation assay of recombinant TAT-Polycomb protein-transduced murine BM cells and tumorigenesis

Murine BM cells exposed to TAT-Polycomb for 48 h were transplanted into 9-Gy-irradiated mice. Hematopoietic cells derived from TAT-Bmi1-transduced BM cells were significantly increased in the peripheral blood at 6 weeks after transplantation (Fig. 3A). The effect of Bmi1 was attenuated after the transplantation of BM cells exposed to both TAT-Bmi1 and TAT-Mel18. Figure 3B shows the flow cytometry analysis of peripheral blood cells from these transplanted mice at 6 weeks after transplantation. Because 80% of mice transplanted with TAT-Bmi1-transduced BM cells died at 8 to 24 weeks after transplantation, we could not perform long-term engraftment analysis. However, only a few early deaths were observed in mice transplanted with BM cells exposed to both TAT-Bmi1 and TAT-Mel18 (Fig. 4A). It is possible that the mice transplanted with BM cells exposed to TAT-Bmi1 died because of cancer, such as leukemia, because *BMI1* is also involved in the malignancy of cancer cells [21–24]. However, we were not able to analyze this before the mice

died. Murine BM cells were exposed to TAT-Polycomb for only 48 h and then cell culturing was continued for 8 weeks with cytokines. However, we detected no morphological malignancies in the cells (Fig. 4B). During cell culturing for 8 weeks, the number of Bmi1-exposed cells was expanded by approximately 500 times the original number of cultured cells (Fig. 4C). Although we could not prove the malignancy of these cells, this phenomenon could represent the proliferation of malignant cells.

#### *Regulation of target gene expression by recombinant TAT-Polycomb proteins in vitro*

We added each TAT-fusion protein to MEL cells every 6 h until 48 h and examined cell proliferation. Cell proliferation increased after the addition of either Bmi1 or Mel18, as assessed by cell growth (Fig. 5A). The cell cycle inhibitory gene *ink4a/arf* is a target of Bmi1. To analyze whether the transduced recombinant Polycomb proteins regulate the expression of their target genes, we performed real-time reverse transcriptase PCR on MEL cells that were cultured for 48 h with TAT-Polycomb at a final concentration of 50 nM. The expression of these genes was inhibited in MEL cells exposed to TAT-Polycomb (Fig. 5B).

#### *Bmi1 and Mel18 are present in distinct complexes*

We previously demonstrated that only a small number of hematopoietic cells simultaneously express *bmi1* and *mel18* [14]. In the present study, we performed a pull-down assay with HisTag to analyze whether Polycomb-group complexes includes both Bmi1 and Mel18.

We did not detect Bmi1, Mel18, or Ring1A in the pull-down assays of protein extracts from MEL cells exposed to TAT-GFP for 6 h using a HisTag-specific resin. However, in the pull-down assay of MEL cells exposed to TAT-Bmi1, Bmi1, and RINGA1A were detected together with a small quantity of Mel18. In contrast, Bmi1 was not detected in MEL cells exposed to TAT-Mel18 (Fig. 5C). These results suggest that PRC1 includes either Bmi1 or Mel18 (Fig. 5D).

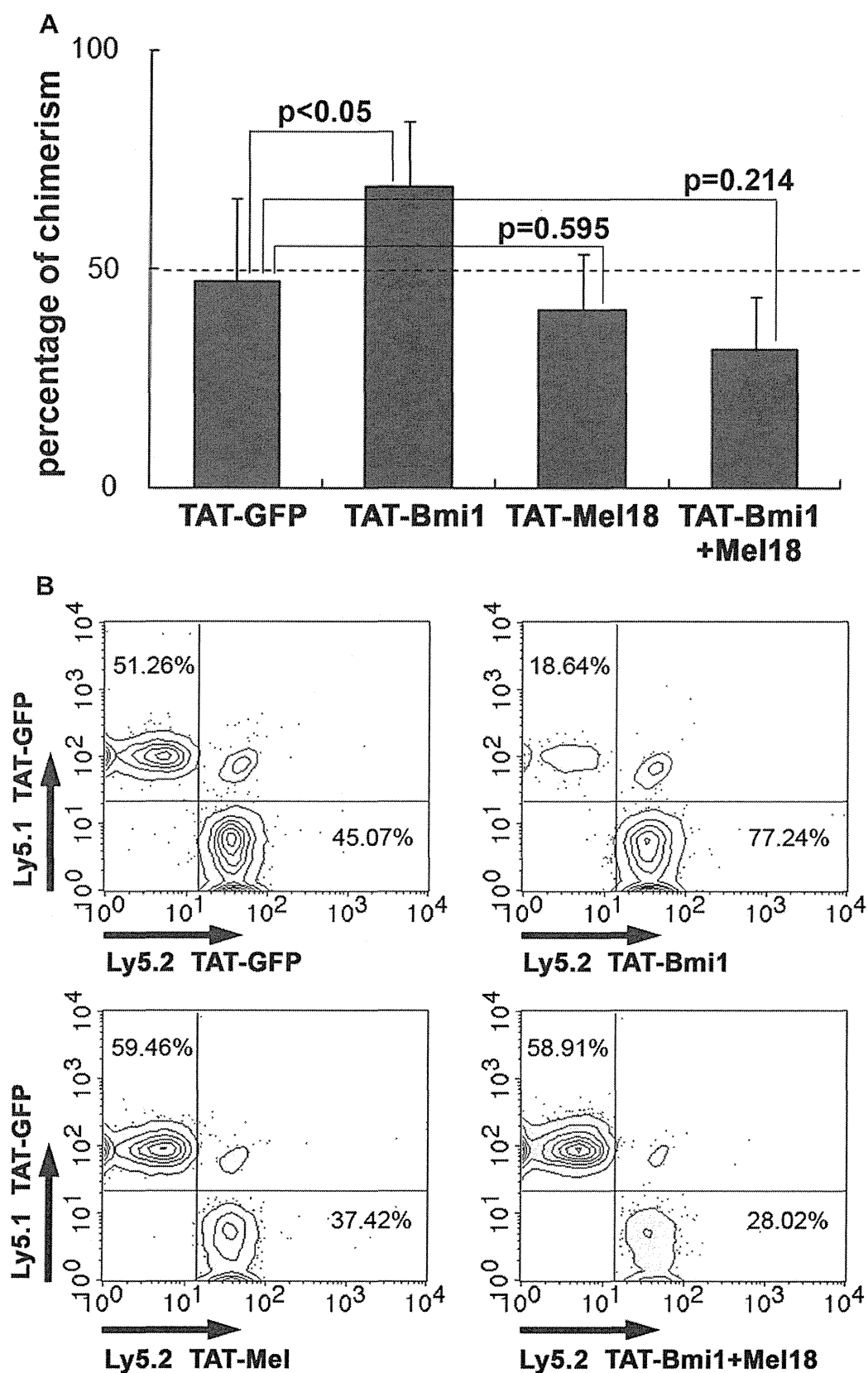


**Figure 3.** In vivo BM transplantation assay of recombinant TAT-Polycomb protein-transduced murine BM cells. (A) Hematopoietic cells derived from TAT-Bmi1-transduced BM cells were significantly increased in the peripheral blood at 6 weeks after transplantation. The effect of Bmi1 was attenuated following the transplantation of BM cells exposed to both TAT-Bmi1 and TAT-Mel18. (B) Flow cytometry profiles of peripheral blood cells from transplanted mice at 6 weeks after transplantation.

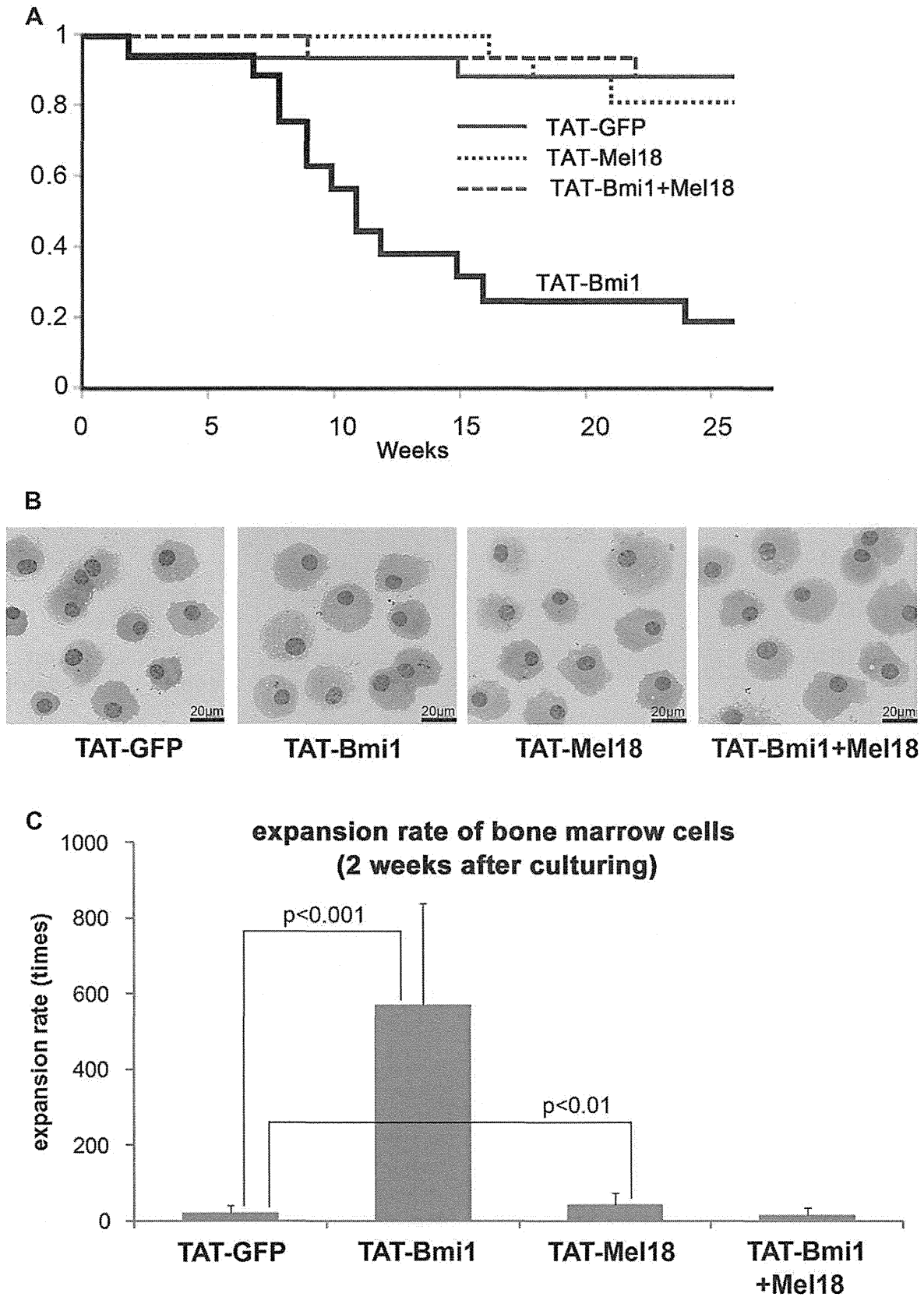


**Figure 4.** Long-term observation of bone marrow (BM) transplantation assay and tumorigenesis. (A) Approximately 80% of mice transplanted with TAT-Bmi1-transduced BM cells died at 8 to 24 weeks after transplantation. (B) BM cells were exposed to TAT-Polycomb for 48 h, and the cells were cultured for 8 weeks in the presence of cytokines. However, we did not observe any morphological malignancies in the cells. (C) However, during cell culture for 8 weeks, the number of Bmi1-exposed cells was expanded by approximately 500 times the original number of cells.

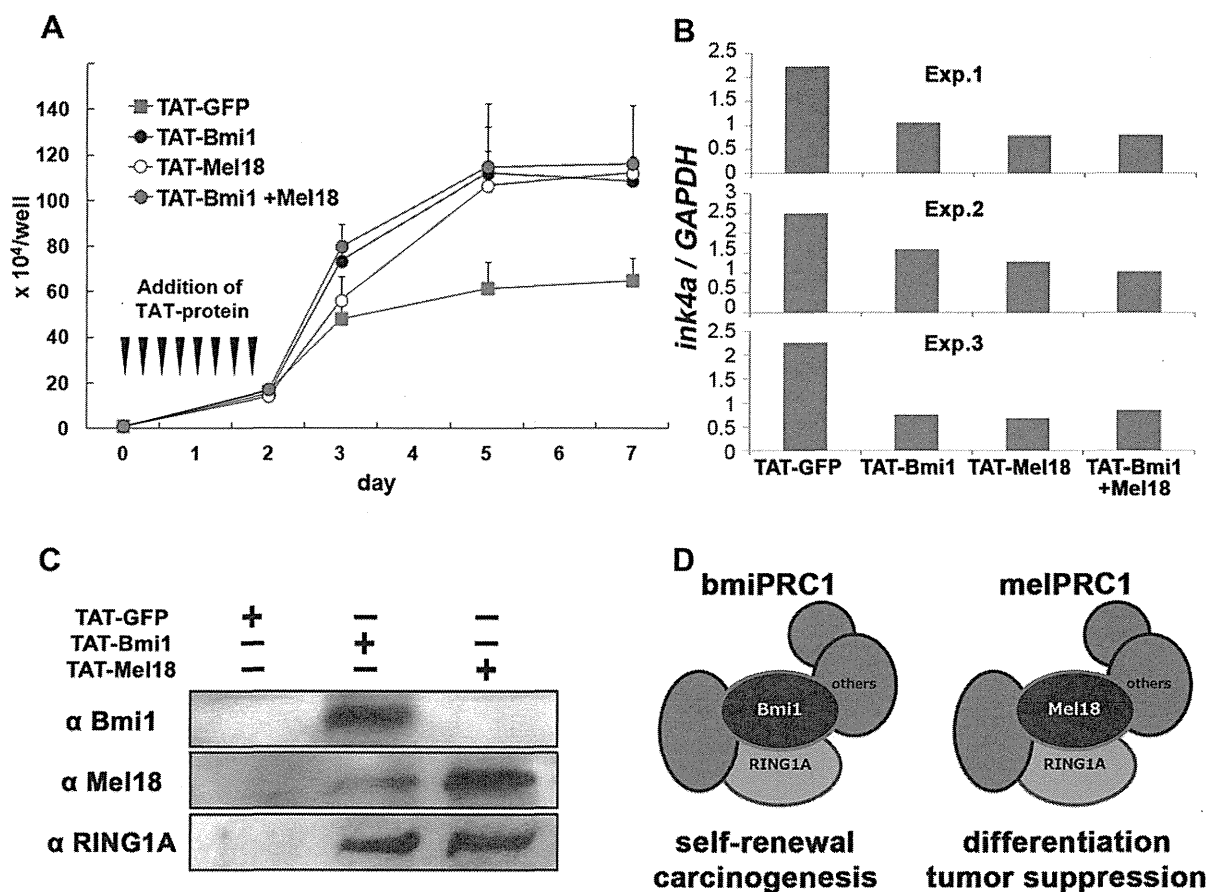


**Figure 5.** Regulation of target gene expression by TAT-Polycomb proteins and the components of PRC1. (A) We added each TAT-fusion protein to MEL cells every 6 h for 48 h and examined cell proliferation. Cell proliferation increased following the addition of either Bmi1 or Mel18. (B) The expression of these genes was inhibited in cells exposed to TAT-Polycomb. (C) A pull-down assay using HisTag was performed to analyze whether Polycomb-group complexes include both Bmi1 and Mel18. In the pull-down assay of MEL cells exposed to TAT-Bmi1, Bmi1, and RING1A were detected together with a small quantity of Mel18. In contrast, Bmi1 was not detected at all in the pull-down assay of MEL cells exposed to TAT-Mel18. (D) Results are summarized in the schema.

## Discussion

Bmi1 is involved in cell proliferation through the negative regulation of *cdkn2a* (*ink4a*), which is one of the major target genes of Bmi1 and cell cycle inhibitory genes [36]. We report that the expression of *ink4a* is inhibited in MEL cells exposed to TAT-Polycomb. We do not consider that the influence of PTD-Polycomb persists for days, and suggest that cell fate was decided within 48 h of exposure to PTD-Polycomb. Despite the opposing functions of Bmi1 and Mel18 in the self-renewal of HSCs, they showed no opposing function in the expression of *ink4a*. Therefore, *ink4a* might not be involved in the regulation of HSC self-renewal by Bmi1/Mel18. However, in the present study, the growth rate differed between BM cells and MEL cells after exposure to TAT-Polycomb. *ink4a* is located downstream of both Bmi1 and Mel18. Because both inhibit cell cycle inhibitors such as *ink4a*, the finding of increase in the number of cells is expected. However, with the BM cell including stem cell, the outcomes differed between Bmi1 and Mel18. Further studies are required to determine the cell type of BM cells that increased after 2-week culture

with exposure to TAT-Bmi1 and the behavior of Polycomb proteins in stem cells and during cancer cell growth.

It has been reported that *bmi1* is essential for the maintenance and self-renewal of stem cells, including hematopoietic, neural, and cancer stem cells [16–20]. Although side population cells in the stem cells of hepatocellular carcinoma expressed *bmi1* preferentially, the number of side population cells decreased after *bmi1* knockdown with RNAi. It was thought that *BMII* contributes to tumorigenesis and prognosis, and the high expression of *BMII* is associated with a poor prognosis [21–24].

Although we expected that HSCs could proliferate after transduction with TAT-Bmi1, we also found a risk of tumorigenesis. In this study, although transplantation of HSCs exposed to TAT-Bmi1 into irradiated mice resulted in the short-term proliferation of hematopoietic cells derived from transplanted HSCs, 80% of the transplanted mice died after 8 weeks. Although we could not analyze the BM of the dead mice, we speculate that the transplanted HSCs exposed to TAT-Bmi1 had transformed into tumors, especially leukemia. Therefore, the probability of developing

leukemia might increase after exposure to Bmi1. The BM of the surviving mice was confirmed to be normal. Interestingly, Mel18 had the potential to inhibit this tumorigenesis; therefore, Mel18 might inhibit the development of cancers involving Bmi1. It is known that *mel18* inhibits tumorigenesis [37]. The tumorigenicity of NIH3T3 cells treated with sense or antisense *mel18* has been analyzed, and it was found that treatment with antisense *mel18* reduces tumor size, probably because of the contribution of *c-myc*. Tetsu et al. proposed that *mel18* negatively regulates the cell cycle through a *c-myc/cdc25* cascade [38].

Previous studies have reported a relationship between Bmi1 and Mel18. Some studies demonstrated the opposing functions of BMI1 and MEL18 in gastric cancer [29] and medulloblastoma. In a medulloblastoma cell line, BMI1 and MEL18 were present in distinct protein complexes [28]. Moreover, we previously reported that the increased expression of *bmi1* and *mel18* is associated with the self-renewal and differentiation of HSCs [14]. One HSC that was undergoing self-renewal or differentiation expressed *bmi1* alone or *mel18* alone, respectively. These reports indicate that *bmi1* and *mel18* have opposing functions in cell proliferation and differentiation. Elderkin et al. reported that MEL18 and BMI1 proteins are components of similar but mutually exclusive PRC1-like complexes in the human 293T cell line [39]. Our results suggest that Bmi1 and Mel18 induce opposite phenomena, which is consistent with these reports. Because Bmi1 and Mel18 are present in distinct complexes, Mel18 may function as an antagonist by inhibiting Bmi1 competitively. Thus, we have demonstrated that PRC1 complexes, including Bmi1 (referred to as *bmiPRC1*) and Mel18 (referred to as *melPRC1*), regulate the self-renewal and differentiation of HSCs, respectively. To investigate the signaling pathway, Guo et al. analyzed the proliferation of human fibroblasts transduced with *Mel18* and *Bmi1* or the knockdown of these proteins with RNAi [26]. They analyzed various molecules involved in the cell cycle and concluded that Mel18 negatively regulates *Bmi1* through *c-myc*. Furthermore, in a study using a breast cancer cell line transduced with *MEL18* and *BMI1* or knockdown of these proteins with RNAi, MEL18 was shown to inhibit Akt, thereby repressing Bmi1 and tumorigenesis [27]. In a recent study, although Akt and Mel18 were in a reverse order, the helix-loop-helix differentiation and DNA binding (Id1) protein enhanced the phosphorylation of Akt and inhibited Mel18, thereby activating *c-myc* and increasing the transcription of *bmi1* [40]. However, because the upstream and downstream signaling pathways remain controversial and the microenvironment affects the regulation of HSC self-renewal, it is commonly recognized that Bmi1 and Mel18 have opposing functions and are present in distinct complexes.

#### Acknowledgments

We thank Professor Y. Takihara (Department of Stem Cell Biology, Research Institute for Radiation Biology and Medicine, Hiroshima

University) for guidance with BM transplantation. We thank Professor M. Kanno (Department of Immunology, Graduate School of Biomedical Sciences, Hiroshima University) for helpful discussions. The murine erythroleukemia cells were a kind gift from Dr. H. Harada (Department of Hematology and Oncology, Research Institute for Radiation Biology and Medicine, Hiroshima University). We thank the Analysis Center of Life Science, Hiroshima University, for allowing us to use their facilities.

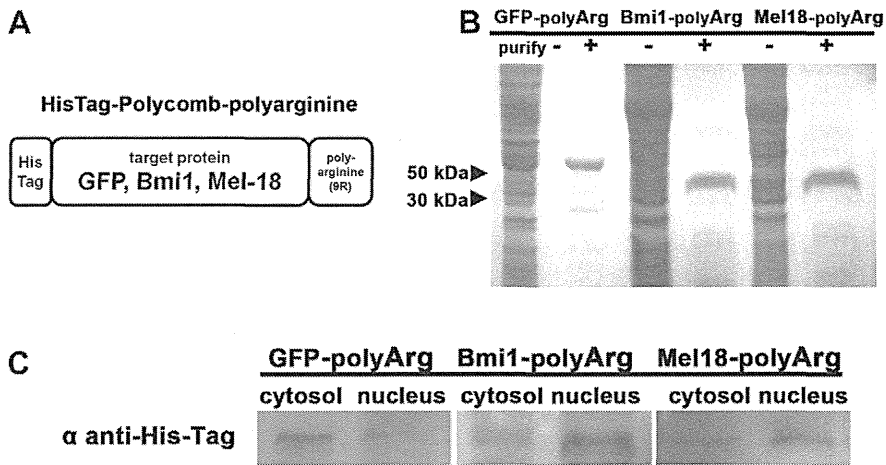
#### Conflict of interest disclosure

No financial interest/relationships with financial interest relating to the topic of this article have been declared.

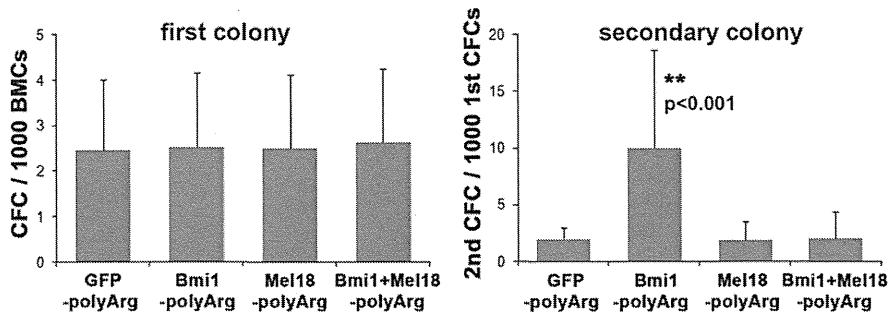
#### References

- Bernstein E, Duncan EM, Masui O, Gil J, Heard E, Allis CD. Mouse polycomb proteins bind differentially to methylated histone H3 and RNA and are enriched in facultative heterochromatin. *Mol Cell Biol*. 2006;26:2560–2569.
- Fischle W, Wang Y, Jacobs SA, Kim Y, Allis CD, Khorasanizadeh S. Molecular basis for the discrimination of repressive methyl-lysine marks in histone H3 by Polycomb and HP1 chromodomains. *Genes Dev*. 2003;17:1870–1881.
- Cao R, Tsukada Y, Zhang Y. Role of Bmi-1 and Ring1A in H2A ubiquitylation and Hox gene silencing. *Mol Cell*. 2005;20:845–854.
- Wang H, Wang L, Erdjument-Bromage H, et al. Role of histone H2A ubiquitination in Polycomb silencing. *Nature*. 2004;431:873–878.
- Alkema MJ, Bronk M, Verhoeven E, et al. Identification of Bmi1-interacting proteins as constituents of a multimeric mammalian polycomb complex. *Genes Dev*. 1997;11:226–240.
- Gunster MJ, Satijn DP, Hamer KM, et al. Identification and characterization of interactions between the vertebrate polycomb-group protein BMI1 and human homologs of polyhomeotic. *Mol Cell Biol*. 1997;17:2326–2335.
- Hashimoto N, Brock HW, Nomura M, et al. RAE28, BMI1, and M33 are members of heterogeneous multimeric mammalian Polycomb group complexes. *Biochem Biophys Res Commun*. 1998;245:356–365.
- Shao Z, Raible F, Mollaaghababa R, et al. Stabilization of chromatin structure by PRC1, a Polycomb complex. *Cell*. 1999;98:37–46.
- Francis NJ, Saurin AJ, Shao Z, Kingston RE. Reconstitution of a functional core polycomb repressive complex. *Mol Cell*. 2001;8:545–556.
- Ohta H, Sawada A, Kim JY, et al. Polycomb group gene *rae28* is required for sustaining activity of hematopoietic stem cells. *J Exp Med*. 2002;195:759–770.
- Iwama A, Oguro H, Negishi M, et al. Enhanced self-renewal of hematopoietic stem cells mediated by the polycomb gene product Bmi-1. *Immunity*. 2004;21:843–851.
- Iwama A, Oguro H, Negishi M, Kato Y, Nakauchia H. Epigenetic regulation of hematopoietic stem cell self-renewal by polycomb group genes. *Int J Hematol*. 2005;81:294–300.
- Kajiume T, Ninomiya Y, Ishihara H, Kanno R, Kanno M. Polycomb group gene *mel-18* modulates the self-renewal activity and cell cycle status of hematopoietic stem cells. *Exp Hematol*. 2004;32:571–578.
- Kajiume T, Ohno N, Sera Y, Kawahara Y, Yuge L, Kobayashi M. Reciprocal expression of Bmi1 and Mel-18 is associated with functioning of primitive hematopoietic cells. *Exp Hematol*. 2009;37:857–866.
- Park IK, Qian D, Kiel M, et al. Bmi-1 is required for maintenance of adult self-renewing haematopoietic stem cells. *Nature*. 2003;423:302–305.
- Lessard J, Sauvageau G. Bmi-1 determines the proliferative capacity of normal and leukaemic stem cells. *Nature*. 2003;423:255–260.
- Hosen N, Yamane T, Muijtjens M, Pham K, Clarke MF, Weissman IL. Bmi-1-green fluorescent protein-knock-in mice reveal the dynamic

- regulation of bmi-1 expression in normal and leukemic hematopoietic cells. *Stem Cells*. 2007;25:1635–1644.
18. Rizo A, Dontje B, Vellenga E, de Haan G, Schuringa JJ. Long-term maintenance of human hematopoietic stem/progenitor cells by expression of BMI1. *Blood*. 2008;111:2621–2630.
  19. Liu S, Dontu G, Mantle ID, et al. Hedgehog signaling and Bmi-1 regulate self-renewal of normal and malignant human mammary stem cells. *Cancer Res*. 2006;66:6063–6071.
  20. Molofsky AV, Pardal R, Iwashita T, Park IK, Clarke MF, Morrison SJ. Bmi-1 dependence distinguishes neural stem cell self-renewal from progenitor proliferation. *Nature*. 2003;425:962–967.
  21. Chowdhury M, Mihara K, Yasunaga S, Ohtaki M, Takihara Y, Kimura A. Expression of Polycomb-group (PcG) protein BMI-1 predicts prognosis in patients with acute myeloid leukemia. *Leukemia*. 2007;21:1116–1122.
  22. Mohty M, Yong AS, Szydlo RM, Apperley JF, Melo JV. The polycomb group BMI1 gene is a molecular marker for predicting prognosis of chronic myeloid leukemia. *Blood*. 2007;110:380–383.
  23. Mihara K, Chowdhury M, Nakaju N, et al. Bmi-1 is useful as a novel molecular marker for predicting progression of myelodysplastic syndrome and patient prognosis. *Blood*. 2005;107:305–308.
  24. Chiba T, Miyagi S, Saraya A, et al. The polycomb gene product BMI1 contributes to the maintenance of tumor-initiating side population cells in hepatocellular carcinoma. *Cancer Res*. 2008;68:7742–7749.
  25. Freemont PS, Hanson IM, Trowsdale J. A novel cysteine-rich sequence motif. *Cell*. 1992;64:483–484.
  26. Guo WJ, Datta S, Band V, Dimri GP. Mel-18, a polycomb group protein, regulates cell proliferation and senescence via transcriptional repression of Bmi-1 and c-Myc oncoproteins. *Mol Biol Cell*. 2007;18:536–546.
  27. Guo WJ, Zeng MS, Yadav A, et al. Mel-18 acts as a tumor suppressor by repressing Bmi-1 expression and down-regulating Akt activity in breast cancer cells. *Cancer Res*. 2007;67:5083–5089.
  28. Wiederschain D, Chen L, Johnson B, et al. Contribution of polycomb homologues Bmi-1 and Mel-18 to medulloblastoma pathogenesis. *Mol Cell Biol*. 2007;27:4968–4979.
  29. Zhang XW, Sheng YP, Li Q, et al. BMI1 and Mel-18 oppositely regulate carcinogenesis and progression of gastric cancer. *Mol Cancer*. 2010;9:40.
  30. Wadia JS, Dowdy SF. Protein transduction technology. *Curr Opin Biotechnol*. 2002;13:52–56.
  31. Michiue H, Tomizawa K, Wei FY, et al. The NH2 terminus of influenza virus hemagglutinin-2 subunit peptides enhances the antitumor potency of polyarginine-mediated p53 protein transduction. *J Biol Chem*. 2005;280:8285–8289.
  32. Kros J, Austin P, Beslu N, Kroon E, Humphries RK, Sauvageau G. In vitro expansion of hematopoietic stem cells by recombinant TAT-HOXB4 protein. *Nat Med*. 2003;9:1428–1432.
  33. Zhou H, Wu S, Joo JY, et al. Generation of induced pluripotent stem cells using recombinant proteins. *Cell Stem Cell*. 2009;4:381–384.
  34. Ikuta K, Weissman IL. Evidence that hematopoietic stem cells express mouse c-kit but do not depend on steel factor for their generation. *Proc Natl Acad Sci USA*. 1992;89:1502–1506.
  35. Li CL, Johnson GR. Murine hematopoietic stem and progenitor cells, I: enrichment and biologic characterization. *Blood*. 1995;85:1472–1479.
  36. Jacobs JJ, Kieboom K, Marino S, DePinho RA, van Lohuizen M. The oncogene and Polycomb-group gene bmi-1 regulates cell proliferation and senescence through the ink4a locus. *Nature*. 1999;397:164–168.
  37. Kanno M, Hasegawa M, Ishida A, Isono K, Taniguchi M. mel-18, a Polycomb group-related mammalian gene, encodes a transcriptional negative regulator with tumor suppressive activity. *EMBO J*. 1995;14:5672–5678.
  38. Tetsu O, Ishihara H, Kanno R, et al. mel-18 negatively regulates cell cycle progression upon B cell antigen receptor stimulation through a cascade leading to c-myc/cdc25. *Immunity*. 1998;9:439–448.
  39. Elderkin S, Maertens GN, Endoh M, et al. A phosphorylated form of Mel-18 targets the Ring1B histone H2A ubiquitin ligase to chromatin. *Mol Cell*. 2007;28:107–120.
  40. Qian T, Lee JY, Park JH, Kim HJ, Kong G. Id1 enhances RING1b E3 ubiquitin ligase activity through the Mel-18/Bmi-1 polycomb group complex. *Oncogene*. 2010;29:5818–5827.



**Supplementary Figure E1.** Preparation of recombinant polyarginine-polycomb proteins. (A) *bmi1*, *mel18*, and *GFP* genes were designed to fuse a poly-arginine to the C-terminal of these three proteins. (B) The recombinant polyarginine-polycomb proteins were purified. Proteins were separated using sodium dodecyl sulfate polyacrylamide gel electrophoresis, and the polyacrylamide gel was stained with Coomassie brilliant blue. (C) Purified polyarginine-polycomb was added to the culture of MEL cells. The MEL cells were separated in nuclear and cytosol. GFP was detected more often in the cytosol than in the nuclear. Bmi1 and Mel18 were detected exclusively in the nuclear.



**Supplementary Figure E2.** In vitro colony assay of recombinant polyarginine-polycomb protein-transduced murine BM cells. Similar to the recombinant TAT-polycomb proteins, the recombinant proteins did not show any significant differences in the primary colony-forming potential. However, BM cells exposed to recombinant poly-arginine-Bmi1 proteins showed an increased number of secondary colonies. In contrast, BM cells exposed to recombinant poly-arginine-Mel18 proteins or to both proteins showed a decreased number of secondary colonies.

## Two cases of partial dominant interferon- $\gamma$ receptor 1 deficiency that presented with different clinical courses of bacille Calmette–Guérin multiple osteomyelitis

Kaoru Obinata · Tsubasa Lee · Takahiro Niizuma ·  
Keiji Kinoshita · Toshiaki Shimizu ·  
Takayuki Hoshina · Yuka Sasaki · Toshiro Hara

Received: 2 May 2012 / Accepted: 21 September 2012  
© Japanese Society of Chemotherapy and The Japanese Association for Infectious Diseases 2012

**Abstract** We experienced two cases of unrelated Japanese children with bacille Calmette–Guérin (BCG) multiple osteomyelitis with partial interferon (IFN)- $\gamma$  receptor 1 (IFNGR1) deficiency. Heterozygous small deletions with frame shift (811 del4 and 818 del4) were detected, which were consistent with the diagnosis of partial dominant IFNGR1 deficiency. Case 1: a 2-year-old boy visited us because of limb and neck pain. He had been vaccinated with BCG at 17 months of age. Multiple destructive lesions were observed in the skull, ribs, femur, and vertebral bones. *Mycobacterium bovis* (BCG Tokyo 172 strain by RFLP technique) was detected in the bone specimen. The BCG multiple osteomyelitis was treated successfully without recurrence. Case 2: an 18-month-old girl developed multiple osteomyelitis 9 months after BCG inoculation. Radiologic images showed multiple osteolytic lesions in the skull, ribs, femur, and vertebrae. *M. bovis* (BCG Tokyo 172 strain) was detected in the cultures from a bone biopsy. Her clinical course showed recurrent osteomyelitis and lymphadenitis with no pulmonary involvement. The

effects of high-dose antimycobacterial drugs and IFN- $\gamma$  administration were transient, and complete remission has since been achieved by combination antimycobacterial therapy, including levofloxacin. Partial dominant IFNGR1 deficiency is a rare disorder, but it should be considered when a patient presents with multiple osteomyelitis after BCG vaccination. The cases that are resistant to conventional regimens require additional second-line antituberculous drugs, such as levofloxacin.

**Keywords** Interferon- $\gamma$  receptor 1 deficiency · Multiple osteomyelitis · Bacille Calmette–Guérin · Mycobacterial infection · Levofloxacin

### Introduction

Interleukin-12 (IL-12)- and IFN- $\gamma$  (IFNG)-mediated immunity plays an important role in host defense against intracellular pathogens [1]. Mendelian susceptibility to mycobacterial disease (MSMD) is a rare disorder and sometimes lethal disease that occurs in response to poorly virulent mycobacteria, such as bacille Calmette–Guérin (BCG) and environmental nontuberculous mycobacteria (NTM). In patients with MSMD, different types of mutations in six genes—IFNGR1, IFNGR2, IL12RB1, IL12B, STAT-1, and NEMO—have been revealed [2].

Sasaki et al. [3] previously reported a partial IFNGR1 mutation in three Japanese children with BCG osteomyelitis and in the father of one of the patients. We have followed the two unrelated cases over 10 years since their onset in the same department (Koshigaya Municipal Hospital). Based on our longitudinal experience, we intend to provide important clinical information for the diagnosis and treatment of IFN- $\gamma$ R1 deficiency in Japan.

K. Obinata · T. Lee · T. Niizuma · K. Kinoshita  
Department of Pediatrics, Koshigaya Municipal Hospital,  
Saitama, Japan

K. Obinata (✉)  
Department of Pediatrics, Juntendo University Urayasu Hospital,  
2-1-1 Tomioka, Urayasu, Chiba 279-0021, Japan  
e-mail: obinata@juntendo-urayasu.jp

T. Shimizu  
Department of Pediatrics, Faculty of Juntendo University,  
Tokyo, Japan

T. Hoshina · Y. Sasaki · T. Hara  
Department of Pediatrics, Graduate School of Medical Science,  
Kyushu University, Fukuoka, Japan



Case report

Case 1

A Japanese boy became spontaneously positive to a tuberculin purified protein derivative (PPD) skin test at the age of 11 months. There was no family history of tuberculosis. A chest X-ray film showed no abnormal findings. The PPD skin test turned negative after 6 months of prophylactic treatment with isoniazid (INH). He was inoculated with BCG (Tokyo 172 strain) by the multiple puncture technique at the age of 17 months. Nine months later (at 26 months of age), he started to limp and could not move his neck. He visited Koshigaya Municipal Hospital, and multiple osteolytic lesions were observed on his skull, vertebrae (cervical and lumbar), ribs, and femur by X-ray, bone scintigram, and magnetic resonance (MR) imaging. *Mycobacterium* was detected in the bone biopsy. *Mycobacterium bovis* was identified as the BCG Tokyo 172 strain by restriction fragment length polymorphism (RFLP). The BCG osteomyelitis was treated successfully with antimycobacterial therapy with isoniazid (INH), rifampicin (RFP), and streptomycin (SM) for 1.5 years without recurrence. He is now 17 years old and has not had a mycobacterial infection since the treatment.

Case 2 (Fig. 1)

An 18-month-old girl (13 years old at present) developed left axillary lymphadenitis 2 months after BCG inoculation at the age of 8 months. Multiple skin eruptions and abscesses appeared 9 months after the vaccination. At the BCG inoculation site, there were signs of hypertrophic scar and keloid. Granuloma was also observed below the

inoculation site. X-ray, skeletal scintigram, and MR imaging showed multiple osteolytic lesions in the skull, ribs, femur, and vertebrae. A bone biopsy specimen of the femur revealed granulomatous inflammation without central necrosis. *M. bovis* (BCG Tokyo 172 strain) was detected in cultures from the bone biopsy by RFLP. She was treated with INH, RFP, and SM, and showed slow improvement. Eighteen months after her initial presentation, she started to develop recurrent osteomyelitis. Additional administration of ethambutol (EB) and IFN- $\gamma$  was effective but the effect was temporary. She exhibited osteomyelitis soon after discontinuation of EB and RFP. High-dose INH and EB, with the addition of clarithromycin (CAM) and IFN- $\gamma$ , proved effective. Her osteomyelitis appeared to have subsided. However, later, at the age of 11 years, she experienced a third relapse of the osteomyelitis. Antimycobacterial therapy was started again, but lymphadenitis also developed on her right supraclavicle. The findings from the swollen lymph nodes were nonspecific. Additional administration of high-dose IFN- $\gamma$  was partially effective against the osteomyelitis and the lymphadenitis. As the cervical lymphadenopathy appeared again, the CAM was changed to levofloxacin (LVFX). A three-drug regimen of INH, RFP, and LVFX for a period of 9 months was successful in achieving remission.

The clinical features of these two unrelated Japanese children with BCG multiple osteomyelitis are summarized in Table 1. Two-color flow cytometric analysis was performed [3] and showed significantly higher levels of IFNGR1 expression on monocytes in both cases. IL-12 and IFN- $\gamma$  production was normal. Genomic DNA was obtained from peripheral blood mononuclear cells. cDNA sequences were analyzed by polymerase chain reaction. Heterozygous small deletions with frame shift (case 1, 811 del4; case 2,

**Fig. 1** Recurrent osteomyelitis and lymphadenitis in case 2. INH isoniazid, RFP rifampicin, SM streptomycin, EB ethambutol, CAM clarithromycin

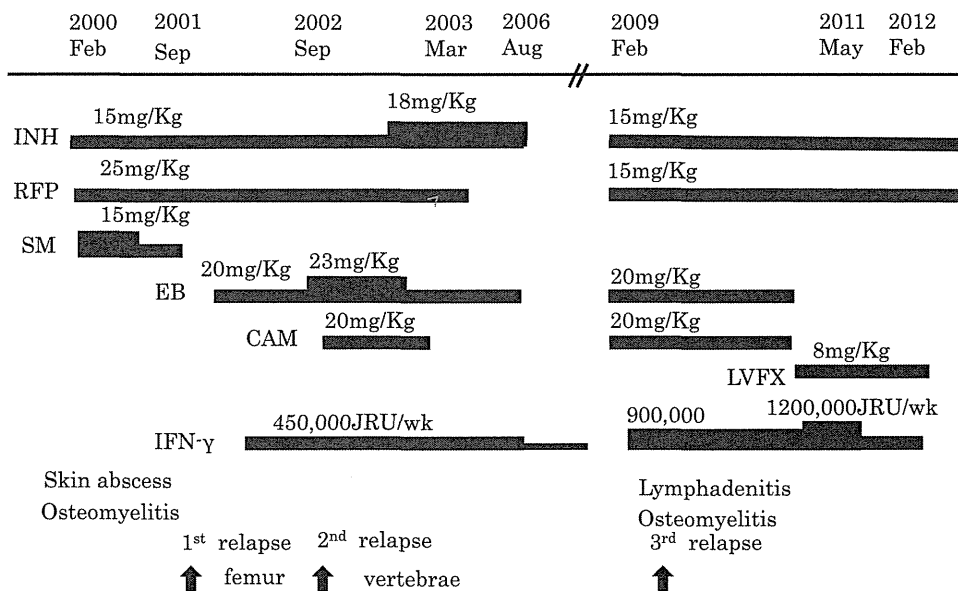


**Table 1** Immunological data at the onset of patients with bacille Calmette–Guérin (BCG) osteomyelitis

Case	1 (17 years/M)	2 (13 years/F)
BCG given at	1 year 5 months	8 months
Age at onset	2 years 2 months	1 year 5 months
Type	Multiple	Multiple, recurrent
Histology	Inflammation	Granuloma
Other organs	None	Skin, lymph node
WBCs/ $\mu$ l	5,300	29,600
Lymphocytes/ $\mu$ l	3,657	7,400
IgG, mg/dl	1,370	1,430
IgA, mg/dl	188	104
IgM, mg/dl	602	181
CD3 cells, %	40.7	56.6
CD4:CD8	3	3
CD19 cells, %	10.4	26.4
PHA response	Normal	Normal
Cytokine production IL-12/INF- $\gamma$	Normal	Normal

818 del4) were detected, which were consistent with the diagnosis of partial dominant IFNGR1 deficiency (data not shown). Sequence analysis of six coding regions was performed and showed that none of the family members of the patients had any mutations. Furthermore, neither sets of parents were consanguineous. Thus, de novo mutation had occurred in both cases 1 and 2.

## Discussion

Bacille Calmette–Guérin vaccines are safe in immunocompetent hosts, and Japanese BCG substrain Tokyo 172 is the safest BCG in the world [4]. Complications of BCG vaccination can be severe and life threatening in infants with immunodeficiency. Systemic adverse reactions to BCG vaccine, including osteomyelitis and disseminated BCG infection, are rare. Toida and Nakata [5] reviewed severe adverse reactions to BCG from 1951 to 2004 in Japan and identified 39 cases (incidence rate, 0.0182 cases per 100,000 vaccinations). Thirteen cases exhibited primary immunodeficiency; 5 of these exhibited chronic granulomatous diseases, 4 exhibited severe combined immunodeficiency, and 4 exhibited IFNGR1 deficiency. Unidentified defects in cellular immunity were observed in 6 cases. The 6 fatal cases had cellular immunodeficiencies. Bone and joint involvement was observed in 27 cases, 15 cases with multiple lesions and 12 cases with single site lesions.

Hoshina et al. [6] analyzed the clinical characteristics and the genetic background of 46 patients with MSMD in

Japan from 1999 to 2009, and found that 6 had mutations in the IFN- $\gamma$ R1 gene. All the cases of IFN- $\gamma$ R1 deficiency exhibited multiple osteomyelitis, and disseminated mycobacterial infection recurred in 5 patients. All the patients exhibited the partial dominant type, and 4 of them had 818 del4. Two of the patients were from the same family, and therefore autosomal dominant inheritance was suspected. The 4 others were considered to have occurred spontaneously. In Taiwan, 3 patients from two unrelated families were identified with a hotspot IFNGR1 deletion mutation (818 del4) and exhibited chronic granulomatous disease-like features, presenting as cutaneous granuloma and multiple osteomyelitis infected with NTM [7]. Fewer patients of Asian origin have been reported with partial dominant IFNGR1 deficiency compared with those of Western countries [8]. The clinical phenotype of partial dominant IFNGR1 deficiency is milder than that of complete deficiency. In this type, BCG and NTM are the major pathogens. Complete IFN- $\gamma$  receptor deficiency is associated with the early onset of severe disease caused by BCG or NTM, whereas the other genetic forms are associated with a milder course of mycobacterial infection [8].

Patients with partial IFGR1 deficiency usually respond well to antibiotic treatment, and for those who do not respond well, additional IFN- $\gamma$  therapy has been shown to be effective [9]. There is no single standard regimen for the treatment of children with BCG osteomyelitis. *M. bovis* is resistant to pyrazinamides because of the expression of a pyrazinamidase. Case 1 was successfully treated with a long-term combination therapy of INH, RFP, and SM. However, in case 2, conventional therapy was inadequate to fight the infection. Additional administration of EB and relatively low dose IFN- $\gamma$  was not able to control the intractable osteomyelitis. As NTM infection was also possible, high-dose EB, INH, and CAM were administered. The regimen was effective but temporary. Combination therapy, including LVFX and high-dose INF- $\gamma$ , was the most successful strategy. Treatment with second-line antituberculous drugs, such as fluoroquinolone, and two first-line drugs (RFP and EB), may be more effective than RFP and EB alone against multidrug-resistant *M. bovis* [10]. LVFX plays an important role as a substitute agent for those patients who are intolerant of first-line antituberculous agents.

IFN- $\gamma$  receptor deficiency is a rare disorder that should be considered when patients exhibit BCG lymphadenitis and disseminated osteomyelitis. Multifocal mycobacterial osteomyelitis without other organ involvement is only seen in dominant partial IFNGR1 deficiency [6, 8]. This type of immunodeficiency tends to exhibit recurrent mycobacterial infection and resistance to conventional antimycobacterial therapy. LVFX is likely an effective option for cases with the partial dominant type that are resistant.

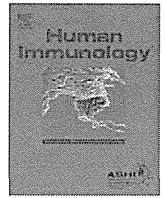
## References

1. Dupuis S, Döffinger R, Picard C, Fieschi C, Altare F, Jouanguy E, et al. Human interferon- $\gamma$ -mediated immunity is a genetically controlled continuous trait that determines the outcome of mycobacterial invasion. *Immunol Rev.* 2000;178:129–37.
2. Filipe-Santos O, Bustamante J, Chaggier A, Vogt G, de Beaucoudrey L, Feinberg J, et al. Inborn errors of IL-12/23- and IFN- $\gamma$ -mediated immunity: molecular, cellular, and clinical features. *Semin Immunol.* 2006;18:347–61.
3. Sasaki Y, Nomura A, Kusuhara K, Takada H, Ahmed S, Obinata K, et al. Genetic basis of patients with Bacille Calmette–Guérin (BCG) osteomyelitis in Japan: identification of dominant partial interferon- $\gamma$  receptor 1 deficiency as a predominant type. *J Infect Dis.* 2002;185:706–9.
4. Milstein JB, Gibson JJ. Quality control of BCG vaccine by WHO: a review of factors that may influence vaccine efficacy and safety. *Bull WHO.* 1990;68:93–108.
5. Toida I, Nakata S. Severe adverse reactions after vaccination with Japanese BCG vaccine: a review. *Kekkaku.* 2007;82:809–24 (in Japanese).
6. Hoshina T, Takada H, Sasaki-Mihara Y, Kusuhara K, Ohshima K, Okada S, Kobayashi M, Ohara O, Hara T. Clinical and host genetic characteristics of Mendelian susceptibility to mycobacterial disease in Japan. *J Clin Immunol.* 2011;31:309–14.
7. Lee W-I, Huang J-L, Lin T-Y, Hsueh C, Wong AM, Hsieh M-Y, et al. Chinese patients with defective IL-12/23-interferon- $\gamma$  circuit in Taiwan: partial dominant interferon- $\gamma$  receptor 1 mutation presenting as cutaneous granuloma and IL-12 receptor  $\gamma$ 1 mutation as pneumatocele. *J Clin Immunol.* 2009;29:238–45.
8. Dorman SE, Picard C, Lammas D, Heyne K, van Dissel JT, Barreto R, et al. Clinical features of dominant and recessive interferon gamma receptor 1 deficiencies. *Lancet.* 2004;364:2113–21.
9. Remus N, Reichenbach J, Picard C, Rietschel C, Wood P, Lammas D, et al. Impaired interferon gamma-mediated immunity and susceptibility to mycobacterial infection in childhood. *Pediatr Res.* 2001;50:8–13.
10. Fennelly GJ. *Mycobacterium bovis* versus *Mycobacterium tuberculosis* as a cause of acute cervical lymphadenitis without pulmonary diseases. *Pediatr Infect Dis J.* 2004;23:590–1.



ELSEVIER

Contents lists available at SciVerse ScienceDirect

journal homepage: [www.elsevier.com/locate/humimm](http://www.elsevier.com/locate/humimm)

## NKRP1A<sup>+</sup> $\gamma\delta$ and $\alpha\beta$ T cells are preferentially induced in patients with *Salmonella* infection

Takayuki Hoshina<sup>a,\*</sup>, Koichi Kusuhara<sup>a,b</sup>, Mitsumasa Saito<sup>a</sup>, Yumi Mizuno<sup>c</sup>, Toshiro Hara<sup>a</sup>

<sup>a</sup> Department of Pediatrics, Graduate School of Medical Sciences, Kyushu University, 3-1-1 Maidashi, Higashi-ku, Fukuoka 812-8582, Japan

<sup>b</sup> Department of Pediatrics, University of Occupational and Environmental Health, 1-1 Iseigaoka, Yahatanishi-ku, Kitakyushu 807-8555, Japan

<sup>c</sup> Fukuoka Children's Hospital and Medical Center for Infectious Diseases, 2-5-1 Tojin-Machi, Chuo-ku, Fukuoka 810-0063, Japan

### ARTICLE INFO

#### Article history:

Received 22 July 2011

Accepted 16 April 2012

Available online 23 April 2012

### ABSTRACT

NKRP1A<sup>+</sup>  $\gamma\delta$  and  $\alpha\beta$  T cells play an important role at the early phase of *Salmonella* infection in mice. Meanwhile, association between NKRP1A<sup>+</sup> T cells and human *Salmonella* infection has not been reported. The objective of this study was to investigate the role of the peripheral NKRP1A<sup>+</sup> T cells in immune response to *Salmonella* infection. Expression of NKRP1A in peripheral  $\gamma\delta$  and  $\alpha\beta$  T cells and production of interferon (IFN)  $\gamma$  and interleukin (IL)-4 in NKRP1A<sup>+</sup>  $\gamma\delta$  and  $\alpha\beta$  T cells were analyzed in 28 patients with acute phase *Salmonella* infection, 23 patients with acute bacterial enterocolitis other than *Salmonella* infection (disease controls) and 44 normal controls by flow cytometry. The proportion of  $\gamma\delta$  T cells expressing NKRP1A and that of IFN $\gamma$ -producing cells in NKRP1A<sup>+</sup>  $\gamma\delta$  cells were significantly higher in *Salmonella* group than those in other two groups. Compared with normal controls, the proportion of  $\alpha\beta$  T cells expressing NKRP1A and that of IL-4-producing cells in NKRP1A<sup>+</sup>  $\alpha\beta$  cells were significantly higher in *Salmonella* group. These data suggested that NKRP1A<sup>+</sup> T cells might play an important role in the early defense mechanism against *Salmonella* infection.

© 2012 American Society for Histocompatibility and Immunogenetics. Published by Elsevier Inc. All rights reserved.

### 1. Introduction

*Salmonella* species form a group of Gram-negative intracellular bacteria, and are common pathogens that cause enterocolitis in humans. The immune response to *Salmonella* infection includes innate immunity comprised of the intestinal epithelium, neutrophils, macrophages, dendritic cells, natural killer (NK) cells, NK T cells and  $\gamma\delta$  T cells, as well as adaptive immunity comprised of antigen-specific T cells and B cells [1–3]. Among the T cell populations,  $\alpha\beta$  T cells express CD4 and/or CD8 and recognize MHC-associated peptides, whereas the majority of  $\gamma\delta$  T cells lack CD4 and CD8 expression and recognize antigens independently of classical MHC class I- or class II-presenting molecules [4]. It was speculated that  $\gamma\delta$  T cells might bridge the innate and adaptive immunity and it was shown that these cells could act as antigen-presenting cells [5,6].

NKRP1A, an NK-cell receptor equivalent to the antigen NK1.1 in mice, is a type II transmembrane C-type lectin-like receptor expressed on the cell membrane as disulfide-linked homodimers [7]. It is expressed on almost all NK and NKT cells, and on a subset of ~25% of CD4<sup>+</sup> T cells [7,8]. Engagement of this receptor modulates several cell functions including cytokine release and transen-

dothelial cell migration [8,9]. NKRP1A<sup>+</sup> T cells secrete several inflammatory cytokines such as IFN $\gamma$  and tumor necrosis factor (TNF)  $\alpha$  [8,10], and also play an immunoregulatory role in several diseases [11,12]. During the early phase of *Salmonella* infection in mice, MHC class II-dependent NK1.1<sup>+</sup>  $\gamma\delta$  T cells are induced to produce IFN $\gamma$ , whereas NK1.1<sup>+</sup>  $\alpha\beta$  T cells are the main source of IL-4 production [13,14]. However, no association between NKRP1A<sup>+</sup> T cells and human *Salmonella* infection has so far been reported.

In the present study, to investigate the role of the peripheral NKRP1A<sup>+</sup> T cells in the human immune response to *Salmonella* infection, we compared the proportion of peripheral  $\alpha\beta$  T cells and  $\gamma\delta$  T cells expressing the NKRP1A molecule and then examined the IFN $\gamma$ - or IL-4-producing cells within the NKRP1A<sup>+</sup>  $\gamma\delta$  and  $\alpha\beta$  T cell populations in patients with acute phase *Salmonella* infection, other non-*Salmonella* bacterial enterocolitis (disease controls) and healthy normal controls.

### 2. Materials and methods

#### 2.1. Subjects

We studied 28 patients with *Salmonella* infection (14 males and 14 females; median age, 6.3 years; range, 1.0–33 years). Stool cultures were carried out for all patients, and blood cultures were carried out for the patients with a fever over 38 °C. The diagnosis of

\* Corresponding author. Fax: +81 92 642 5435.

E-mail address: [hoshina@pediatr.med.kyushu-u.ac.jp](mailto:hoshina@pediatr.med.kyushu-u.ac.jp) (T. Hoshina).